Journal of Photochemistry & Photobiology, B: Biology 186 (2018) 137–143

Contents lists available at ScienceDirect

Journal of Photochemistry & Photobiology, B: Biology

journal homepage: www.elsevier.com/locate/jphotobiol

In vivo photoinduced [4 + 2] dimerization of a *neo*-clerodane diterpene in *Baccharis flabellata*. ROS and RNS scavenging abilities

Matías Funes, Carlos E. Tonn, Marcela Kurina-Sanz*

INTEQUI-CONICET, Facultad de Química, Bioquímica y Farmacia, Universidad Nacional de San Luis, Almirante Brown 1455, CP 5700, San Luis, Argentina

ARTICLE INFO

Keywords:
[4 + 2] cycloaddition
Furan *neo*-clerodane
RNS
ROS

ABSTRACT

Secondary metabolites play a major role in the adaptation of plants to the environment. Furan *neo*-clerodane diterpenes are characteristic secondary metabolites in *Baccharis flabellata* Hook. & Arn. var. *flabellata*. One of the main compounds is the diene *ent*-15,16-epoxy-19-hydroxy-1,3,13(16),14-clerodatetraen-18-oic acid (DAC). In this work a new dimeric compound (DACD) has been isolated and identified by NMR and MS techniques. The presence of other minor dimers was also observed in the same plant methanolic extracts. Assuming that they may be the products of [4 + 2] condensation of two monomeric moieties, the formation of adducts by photochemical dimerization was checked by inducing the *in vitro* [4 + 2] cycloaddition of DAC. Moreover, the DAC and DACD accumulation rates in aerial parts of *B. flabellata* specimens were analyzed monthly during a complete phenological cycle. The accumulation of monomer depends on the plant phonological stage; meanwhile the dimer proportion arises in detriment of the monomer as the solar UV radiation increases. Since plants exposed to strong UV intensities produce radical species, the scavenger properties of these compounds toward reactive nitrogen species (RNS), and reactive oxygen species (ROS), were analyzed. Albeit DAC and DACD show significant superoxide radical scavenger activities, the monomer proved to be more effective than the dimer toward ROS, while DACD was an excellent RNS scavenger.

1. Introduction

Baccharis genus belongs to Asteraceae family and has > 500 species. It is widely spread in South America and clerodane diterpenes are its most representative secondary metabolites [1–3]. Particularly, the diene-acid clerodane *ent*-15,16-epoxy-19-hydroxy-1,3,13(16),14-clerodatetraen-18-oic acid (DAC) was isolated from *Baccharis flabellata* Hook. & Arn. var. *flabellata* [4,5] and from aerial parts of *Dodonaea attenuata* A. Cunn. (Sapindaceae) [6]. Several biological properties have been attributed to *neo*-clerodanes such as antitumor [7], anti-inflammatory [8], antifeedant, insecticide [9,10], and antinociceptive [11].

Although some authors support the idea that natural products appear to have gained complexity from dimerization processes that could take place with a high degree of spontaneity [12], diterpenoid dimers are a rather uncommon subclass of terpenes. Four clerodane dimers linked *via* a C-18 malonate ester were reported in plants of Asteraceae family, specifically from aerial parts of *Baccharis lejia* [13]. Another dimer, synthetized probably due to a [2 + 2] condensation of two monomeric moieties catalyzed either by photo- or enzymatic activity, was reported in *Croton euryphyllus* [14].

Since plants are vulnerable to solar UV radiation, metabolite synthesis as well as other functions could be affected along the year due to differences in sunlight intensity [15,16]. Excessive UV radiation leads to the overproduction of reactive nitrogen species (RNS) and reactive oxygen species (ROS) in plants [17,18]. These reactive species can attack biomolecules such as lipids, proteins and DNA, causing tissue photo-damage. Consequently, to counter the redox imbalance, plants biosynthesize some metabolites to act as scavenger molecules. An example of this was shown by Zhang et al. [19] who demonstrated that UV-B irradiation meaningfully increased NOS activity, NO release and biosynthesis of flavonoids in *Betula pendula* Roth leaves.

In the present work we report the presence of a new furan *neo*-clerodane dimer, DACD, from the aerial parts of the wild bush *B. flabellata* Hook. & Arn. var. *flabellata*. We also assessed the accumulation of both, DAC and its dimer (DACD) in correlation with solar UV radiation intensity. Taking into account the variation of the DAC and DACD rates throughout the different months of the year, RNS and ROS scavenging properties of both compounds was analyzed.

* Corresponding author at: INTEQUI CONICET-UNSL, Almirante Brown 1455, CP 5700 San Luis, Argentina.
E-mail address: mkurina@unsl.edu.ar (M. Kurina-Sanz).

https://doi.org/10.1016/j.jphotobiol.2018.06.020
Received 7 April 2018; Received in revised form 29 June 2018; Accepted 30 June 2018
Available online 09 July 2018
1011-1344/

2. Materials and Methods

2.1. General Experimental Procedures

Solvents used were of analytical grade or were purified by standard procedures prior to use. Silica gel GF254 and Silica gel 60 (0.040–0.063 mm), Alumina Activity II-III (Brockmann), and powdered activated charcoal were purchased at Merck (Darmstadt, Germany). ^{1}H and ^{13}C NMR spectra were performed on a Bruker AC-200 spectrometer (200.13 MHz and 50.23 MHz, respectively) in deutherochloroform ($CDCl_3$). 2D NMR spectra were measured using standard Bruker software. Chemical shifts were referenced to tetramethylsilane (TMS). Electron impact mass spectra (EIMS) were run at 70 eV on GCQ Plus instrument. UV–Vis absorption spectra were taken with a spectrometer Lambda 25 Perkin Elmer (Madrid, Spain). Riboflavin (Rf), ascorbic acid (AA), sodium nitroprusside (SNP), sodium nitrite (SN), Griess reagent kit (GR) and 2,2-diphenyl-1-picrylhydrazyl (DPPH), were purchased from Sigma-Aldrich, Argentina. Compounds were analyzed by HPLC-PDA-ESI-MS/MS, using an Agilent Series 1200 LC System (Agilent, Santa Clara, CA, USA), coupled to a PDA detector (Agilent Series 1200) in tandem with an ESI source, connected to a Micro-QTOF II (Bruker Daltonics, Billerica, MA, USA) mass spectrometer (MS and MS/MS). The HPLC system was equipped with a binary gradient pump, solvent degasser, and autosampler (Agilent Series 1200 L, Santa Clara, CA, USA).

2.2. Plant Material and Isolation of neo-Clerodanes

A well-established wild colony of *B. flabellata* located in a selected parcel at 1270 MASL in Potrero de los Funes, San Luis, Argentina (33° 11′ 90.88″ S, 66° 15′ 42.63″ W) was chosen to perform the present study. In a personal communication Prof. H. Ulacco from Geochemistry and Soils Laboratory from the UNSL Department of Geology classified the soil as sandy-loam non saline, with low electrical conductivity and neutral pH. Leaves and stems (500 g of fresh weight) were collected during the month of December. One specimen was deposited in the Herbarium of the National University of San Luis (UNSL voucher number L.A. Del Vitto & E.M. Petenatti # 9436). Aerial plant parts were chopped and extracted with methanol (MeOH) (4.0 L, twice) at room temperature. The vacuum concentrate methanol extract was subjected to a novel flash chromatography procedure using a combined stationary phase constituting successive layers of alumina (upper layer), activated charcoal (middle layer) and silica gel 60 (lower layer) (150 g each), in order to retain chlorophylls, flavonoids and waxes, in a single procedure. Elution was performed with ethyl acetate (EA). The organic eluate, enriched in terpene compounds, was dried under vacuum yielding 148.7 mg of solid material that was resuspended in 10 mL of MeOH and further separated by preparative centrifugal thin layer chromatography (CTLC) on a Chromatotron (Model 7924T Harrison Research, Palo Alto, CA, USA). The CTLC plates were coated with a 2 mm thick layer of silica gel GF254 (Merck). The mobile phases used were increasing polarity mixtures of *n*-hexane (100%) to EA (100%) that were pumped at a flow-rate of 1 mL min^{-1}. UV detection was carried out at 254 nm and 2 mL fractions were collected. Two terpene compounds, namely DAC (50.1 mg) and DACD (30.2 mg) were obtained as pale-yellow oils.

2.3. NMR Analyses

DAC, *ent*-15,16-epoxy-19-hydroxy-1,3,13(16),14-clerodatetraen-18-oic acid, physical constants as well as spectrometric data were in total agreement with the ones published by Saad et al. and Payne & Jefferies [5,6]. More information is provided in supplementary data SI, Table S1 and Figs. S1, S2 and S3. To assure solubility in $CDCl_3$, DACD and DAC were derivatized with Ac_2O/Py/DMAP, getting a pale-yellow oil.

2.3.1. ^{1}HNMR Spectral Data of DACD-diacetate

δ 7.33 (dd, J = 3.0; 2.0 Hz, H-15′), 7.26 (m, H-3′), 7.18 (br t, H-3), 7.18 (br t, H-16′), 6.22 (m, H-1), 6.22 (m, H-2), 6.22 (m, H-14′), 5.75 (t, J = 3.0 Hz, H-14), 4.54 (d, J = 11.0 Hz, H-19′), 4.47 (d, J = 11.0 Hz, H-19), 4.14 (d, J = 11.0 Hz, H-19), 4.08 (m, H-15), 4.01 (t, J = 5.0 Hz, H-16), 2.82 (m, H-10), 2.55 (m, H-2′), 2.51 (m, H-10′), 2.30 (m, H-12′), 2.20 (m, H-12), 2.05 (s, $-CH_3$ (2 Ac)), 1.80 (m, H-11′), 1.67 (m, H-1′), 1.58 (m, H-11), 1.53 (m, H-8′), 1.50 (m, H-8), 1.30–1.10 (m, H-6), 1.30–1.10 (m, H-7), 1.30–1.10 (m, H-6′), 1.30–1.10 (m, H-7′), 0.89 (d, J = 6.0 Hz, H-17′), 0.81 (d, J = 6.0 Hz, H-17), 0.60–0.50 (s, H-20), 0.60–0.50 (s, H-20′).

2.3.2. ^{13}CNMR Spectral Data of DACD-diacetate

δ 172.1 (2C═O (Ac)), 171.2 (C-18), 171.2 (C-18′), 143.1 (C-3′), 142.7 (C-16′), 138.4 (C-15′), 138.3 (C-4′), 136.3 (C-13), 135.7 (C-1), 134.5 (C-4), 130.2 (C-3), 128.5 (C-14), 125.0 (C-13′), 122.5 (C-2) 110.8 (C-14′), 67.6 (C-19), 62.2 (C-19′), 48.0 (C-15), 47.6 (C-10), 47.5 (C-16), 46.5 (C-10′), 40.6 (C-9), 40.9 (C-9′), 39.2 (C-5′), 38.5 (C-5), 38.3 (C-2′), 38.3 (C-11′), 37.8 (C-11), 36.2 (C-8′), 35.4 (C-8), 33.4 (C-1′), 32.5 (C-6′), 31.0 (C-6), 27.1 (C-7′), 26.9 (C-7), 18.3 (C-12′), 18.2 (C-12) 18.1 (C-17′), 18.0; 16.9 (CH_3 (Ac)), 16.9 (C-17), 15.5 (C-20′), 15.3 (C-20).

2.4. HPLC–DAD Characterization and Validation of DAC and DACD

2.4.1. Characterization of DAC and DACD

A binary pump Waters® 1525 HPLC system (Milford, Massachusetts., USA) attached to a Waters® 2998 UV photodiode array detector working at the range of 200 nm to 750 nm was employed for analytical measurements. DAC and DACD methanol standard solutions (10 mg mL^{-1}) were filtered through a Durapore® syringe membrane (Merck Millipore, Darmstadt, Germany) of 13 mm diameter and 0.22 μm pore size prior to the injection of 10 μL into the HPLC-DAD system. A Chrompack® (packing material: Chromspher® C18, 150 × 4.6 mm diameter, Santa Clara, California, USA) column was used at room temperature. Mobile phase consisting of MeOH 0.1% p/v aqueous acetic acid solution, in a proportion of 7:3 *v*/v, was used for isocratic elution at a flow rate of 1 mL min^{-1}. Total run time was 30 min and the detector was set at 296 nm. Five points calibration curves from each pure compound were obtained in triplicate from stock MeOH solutions. (See chromatograms and UV–vis spectra in SI, Figures: S17–S20).

2.4.2. Validation Method

Linearity, limit of detection (LOD) and limit of quantification (LOQ), precision and accuracy were validated toward pure DAC and DACD samples. Linearity of calibration curves was established by calculating the slope, intercepts and R^2 co-efficient. The regression equation and R^2 (0.99–1) showed good linearity response in the range between 10.0 and 50.0 μg mL^{-1}. LOD and LOQ were calculated as 3.3 σ/S and 10 σ/S respectively, σ being the response standard deviation, and S the slope of each marker. Intra- and inter-day variability test was determined three times within 1 day and 3 on separated days at three different concentrations, respectively. Variations were expressed by the relative standard deviations (RSD) confirming the precision of the proposed method. Also, three concentrations of pre-analyzed sample solutions were spiked with known quantities of the standards and injected in triplicate to perform recovery studies. The percentage recovery of DAC and DACD were between 90.6 and 106.6% (RSD < 4%, n = 3), confirming the accuracy of the proposed method. (See Validation plots in SI, Tables S4 and S5).

2.5. DAC and DACD Accumulation in B. fabellata Aerial Parts

Aerial parts of *B. flabellata* (100 g) were harvested from the above specified parcel every 15th day of each month from March 2016 to February 2017. The biomass was chopped and extracted with MeOH (200 mL) at room temperature for five days. The solvent was evaporated under reduced pressure and 0.3 g of the residue was dissolved in

5 mL of MeOH. Each extract was cleaned-up as described in Section 2.2. and every terpene-enriched sample (10 μL) was injected in the HPLC-DAD system. Furan *neo*-clerodanes were quantified using the corresponding calibration curves. The solar UV radiation values in the field, for each harvesting time, were registered using an Eppley UV photometer (Rhode Island USA) whereas the global irradiances were measured with a pyranometer (Kipp-Zonem model CM-6).

2.6. [4 + 2] Photocycloaddition of DAC under Laboratory Conditions

DAC methanolic solution (1 mM) was degassed under a N_2 stream and 2 mL solution was placed in a quartz cuvette (10 mm i.d.). The solution was irradiated with a germicidal lamp (General Electric GE T8–Germicidal (G36T8)) at 298 K for 8 h. Samples were taken every 2 h and analyzed by HPLC-DAD. A parallel procedure was carried out in the dark at different temperatures ranging between 20 °C and 80 °C.

2.7. Scavenging Assays

2.7.1. Scavenging of DPPH Radical

Free radical scavenging activity was measured using the 2,2-diphenyl-1-picrylhydrazil (DPPH) assay [20]. DAC and DACD sample stock solutions (0.01 M) were prepared in MeOH and 2.5 mL of these were mixed with 1.0 mL of 0.01 M DPPH in MeOH solution at room temperature. After 30 min, absorbance at 518 nm was measured and expressed as antioxidant activity percentage (AA) using the following formula: AA % = [(absorbance of the control – absorbance of the sample)/absorbance of the control] × 100. Control solutions of DAC and DACD (0.01 M) and DPPH 0.1 M in MeOH were used as negative controls. Ascorbic acid (0.01 M) in methanol was used as positive control. Assays were carried out in triplicate.

2.7.2. Superoxide Anion Radical ($O_2\cdot^-$) Scavenging Assay

To evaluate the $O_2\cdot^-$ scavenging potential of DAC and DACD, the delay in riboflavin (0.06 mM aqueous solutions at pH 7.0) photodegradation was measured. Solutions of DAC and DACD (0.06 mM) were used. 10 mM of both hydrazine and mannitol were added as deactivators of singlet oxygen and hydroxyl radical respectively. Continuous photolysis of riboflavin was performed in a home-made photolyser with a 300 W quartz-halogen lamp and a cut-off filter at 360 nm. Riboflavin relative photodegradation rates were obtained from the initial slopes of the absorbance decrease at 446 nm upon 12 min of irradiation in 1 cm × 1 cm cuvettes. Estimated error in the slope values was ± 5%.

2.7.3. Singlet Oxygen ($^1O_2$) Scavenging Assay

The delay in the photodegradation of riboflavin was used to determine the scavenging potential of DAC and DACD over $^1O_2$. Riboflavin MeOH solutions (0.06 mM) were poured in 2 mL, 1 cm path length quartz cells containing DAC or DACD (0.01 mM) and irradiated in the range of 295–385 nm. Absorbances were registered at 446 nm. The observed rate constants (k_{obs}) were calculated by linear least-squares fit of the semilogarithmic plot of Ln A0/A or Ln F0/F *vs* time. Riboflavin methanolic solutions without terpenes were used as reference. All the experiments were performed at 25 °C. The pooled standard deviation of the kinetic data, using different prepared samples, was < 10%.

2.7.4. Nitric Oxide Radical Scavenging Assay

DAC and DACD nitric oxide radical scavenging activities were determined by Garrat method [21]. Briefly, 2 mL of pH 7.4 SNP (10 mM) solution were mixed with 0.5 mL of DAC, DACD or AA solutions to get final concentrations ranging from 10 to 160 μg mL^{-1}. After incubation at 25 °C for 150 min, 0.5 mL of each sample was taken and mixed with 0.5 mL of Griess reagent kit and incubated at room temperature for 30 min. The absorbances were measured at 540 nm.

3. Results and Discussion

3.1. Extraction and Characterization of Furan Diterpenes from Aerial Parts of B. flabellata

3.1.1. Extraction and Purification

The phytochemical re-study of aerial parts of *B. flabellata* here reported was restricted to the terpene fraction, thus chlorophylls, flavonoids and waxes were removed from the methanol extracts by flash chromatography. From the terpene enriched fraction two main compounds namely DAC and DACD were detected by TLC analysis and further purified by CTLC. Both, DAC and DACD, were recovered as a pale-yellow oils.

3.1.2. DAC Spectrometric Characterization

DAC showed an acidic behavior toward a bromothymol blue solution. Its UV spectra performed in methanol and *n*-hexane showed λ_{max} values at 296 and 292 nm [5], respectively, in accordance with the presence of a diene moiety. In order to confirm its identity ^1H NMR and ^{13}C NMR experiments were carried out. All the signals agreed with the ones reported for the furan *neo*-clerodane known as *ent*-15,16-epoxy-19-hydroxy-1,3,13(16),14-clerodatetraen-18-oic acid by Payne & Jefferies in 1973 [6] and Saad et al. in 1987 [5] (Fig. 1).

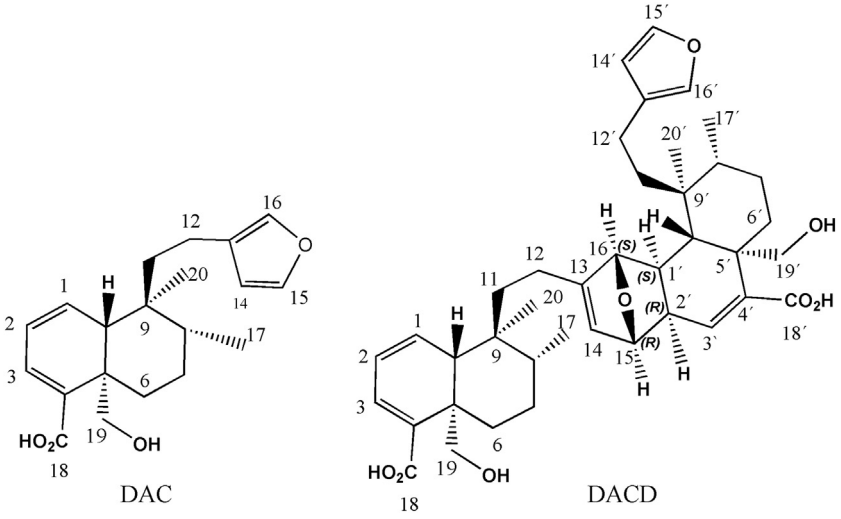

Fig. 1. DAC and DACD structures.

3.1.3. DACD Spectrometric Characterization

DACD should be subjected to peracetylation in order to achieve a good solubility in $CDCl_3$ previous to the NMR studies. The ^1H NMR spectrum of this DACD derivative showed the typical signals corresponding to a β-substituted furan ring at δ 6.22 (1H, m, H-14′); 7.33 (1H, dd, J = 3.0, 2.0 Hz, H-15′) and 7.18 (1H, br t, H-16′) as well as signals which were in agreement with the α,β,γ δ-unsaturated carbonyl system which include C-18, C-4, C-3, C-2, and C-1 moiety. This system showed resonance at δ 6.22 (2H, m) and 7.18 (1H, br t) ppm. Taking into account the presence of two secondary methyl groups (H-17 and H-17′) at δ 0.81 (3H, d, J = 6.0 Hz) and 0.89 (3H, d, J = 6.0 Hz), respectively, and two quaternary methyl groups (H-20 and H-20′) as a pair of singlets between 0.50 and 0.60 ppm (3H each), and considering the molecular weight observed from the HPLC-MS-MS spectrum, we suggest a dimeric structure. Also, the ^{13}C NMR spectrum showed a number of signals that match with this assumption. We propose that the furan ring moiety of one DAC monomer is attached to the C-1 and C-2 double bond of the other monomer (Fig. 1). The configuration of the new stereogenic centers (C-1′, C-2′, C-14, and C-15) formed during the reaction is shown in Fig. 1. This arrangement is the result of the approximation of the furan moiety toward the β-face of the double bond which acts as dienophile. The methylhydroxy group located on C-19 of the monomer has a significant steric hindrance for a suitable approach for the other phase of the decaline moiety (Fig. 2).

Besides in HPLC-MS-MS studies, DACD showed an important peak at m/z 547.3766 which was consistent with the loss of a m/z 95 fragment typical in clerodane diterpenes possessing the β-ethylfurane moiety, accompanied by the loss of a water molecule. To the best of our knowledge, this dimeric compound has not been previously reported by other authors.

3.1.4. DAC and DACD HPLC Analysis

This is also the first report of the establishment of a HPLC–DAD method for DAC and DACD chromatographic characterization. Moreover, as it was described in the Section 2.4.1 and SI, quantification method was validated and further applied to quantify both metabolites in complex methanolic extracts (see SI).

3.2. Accumulation of DAC and DACD in B. fabellata Aerial Parts throughout a Complete Phenological Cycle

In order to determine the variations in monomer and dimer concentrations throughout the course of the year, we decided to assess DAC and DACD accumulation in correlation with the season and therefore plant phenological state. With a monthly frequency, to complete a phenological cycle, the same quantity of plant material was collected from specimens from the same parcel (Section 2.5). The methanolic extracts were cleaned-up by flash chromatography as described in Section 2.2, and further analyzed by HPLC-DAD. Retention times were 9.8 and 17.4 min for the monomer and the dimer, respectively. Representative chromatograms are shown in SI.

Table 1
DAC and DACD accumulation in *B. flabellata* aerial parts along a complete phenological cycle.

Month of collection (Year)	Phenological stage	Extract (g Kg^{-1} plant fresh material)	Solar UV radiation (mJ/m^2)	Concentration (mg Kg^{-1} plant fresh material)	
				DAC	DACD
March (2016)	vegetative	91.2	8.4	80.43	25.44
April (2016)	vegetative	53.7	11.9	2.05	2.48
May (2016)	vegetative	65.3	9.0	4.22	3.95
June (2016)	vegetative	97.4	8.4	6.01	5.72
July (2016)	vegetative	100.6	9.6	24.09	8.32
August (2016)	vegetative	105.4	10.3	36.89	15.70
September (2016)	vegetative	88.1	14.6	25.62	20.25
October (2016)	flowering	75.8	19.6	8.17	80.34
November (2016)	flowering	90.9	23.1	15.17	120.21
December (2016)	full flowering	96.8	24.8	7.27	137.80
January (2017)	fruiting	121.1	23.0	1.02	1.54
February (2017)	fruiting	82.5	20.5	1.63	1.28

In autumn and winter (April–July), when plants are in vegetative stage and the intensity of solar radiation is low, no terpenes were evident in *B. fabellata* aerial parts. In August, at the end of winter, terpenes began to accumulate. The most significant peak area corresponded to the monomer. Other peaks, very likely corresponding to another dimmer different to DACD, increased earlier than DACD peak. As the spring season progressed, DACD concentration augmented while DAC concentration diminished. The maximum DACD level was reached in summer time (December) when plants were in full flowering stage. Variations in the accumulation of DAC and DACD during the complete phenological cycle and their correlation with light intensity are shown in Table 1.

Interestingly, in the fruiting stage, neither the monomer nor the dimer was detected in significant amounts, although the solar radiation index was high. We may assume that during the early flowering stages (November–December), DACD reaches its maximum concentration to protect the seeds, from solar radiation. On the contrary, during fruiting, the plant invests most of its metabolic energy in fruit maturation, in detriment of the biosynthesis of secondary metabolites. At the end of summer (March), once the seeds are dispersed, the plant would be able to prepare itself for a new cycle and restart the synthesis of secondary metabolites.

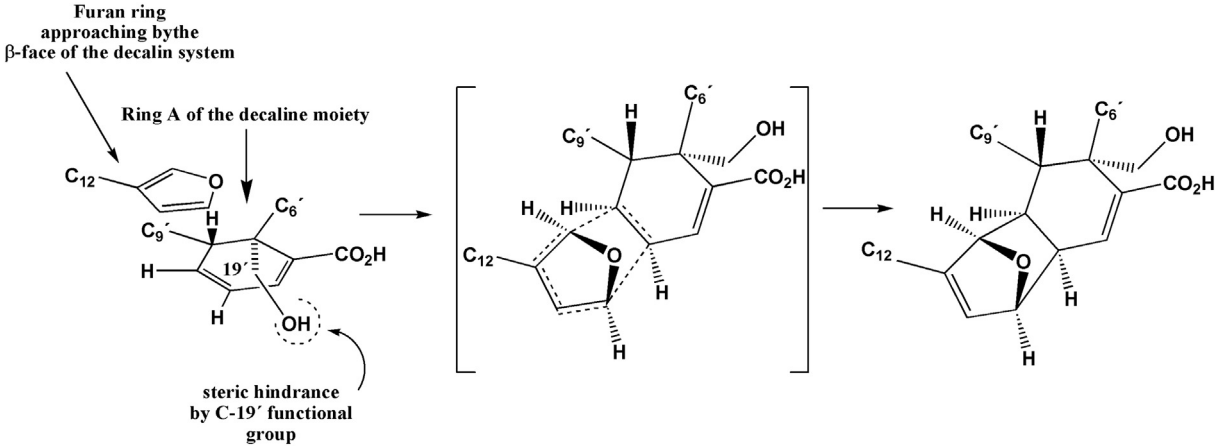

Fig. 2. Probable diene/dienophile approximation in DAC dimerization process.

Undoubtedly, *B. flabellata* plants accumulate different quantities and ratios of furan clerodane compounds depending on the season. Table 1 clearly shows that, in the presence of monomer, the dimer proportion arises in detriment of the monomer as the solar UV radiation increases.

3.3. [4 + 2] Photocycloaddition of DAC

Photocycloaddition [4 + 2] occurs by photo-activation of a diene or a dienophile. An electronically excited molecule is produced and subsequently trapped by the other reagent. Biosynthetic [4 + 2] cycloadditions can occur by enzymatic catalysis also [22]. The fact that adducts of vegetal origin are sometimes isolated as diastereomeric mixtures is in line with a non-enzymatic process. On the other hand, regio- and diastereoselectivity are not conclusive evidences of enzymatic reactions. In the present work, in addition to DACD, other minor compounds showing molecular weights that match with dimers were detected in the methanolic extracts, although their structures could not be elucidated due to their scarce amounts. This suggests that other dimerization processes might be occurring in *B. flabellata* leaves.

To reliably check if DACD comes from DAC dimerization we performed an [4 + 2] photocycloaddition of DAC in methanolic solution under germicidal light. The full experiment lasted 8 h, and samples were taken every 2 h. The dimer signal appeared in the first sample and its concentration increased throughout the experiment in detriment of the monomer quantity (Fig. 3). Interestingly when the same procedure was carried out in the dark at 80 °C, DAC was recovered untransformed. This could be considered as evidence that the formation of DACD is not the result of an intermolecular Diels-Alder thermal [4 + 2] cycloaddition reaction. Nevertheless, the possibility of accessing to dimers by photocatalysis does not rule out the probability that their presence in specific plant phenological stages are due to enzymatically catalyzed reactions. The activity of natural Diels–Alderases that catalyzes the

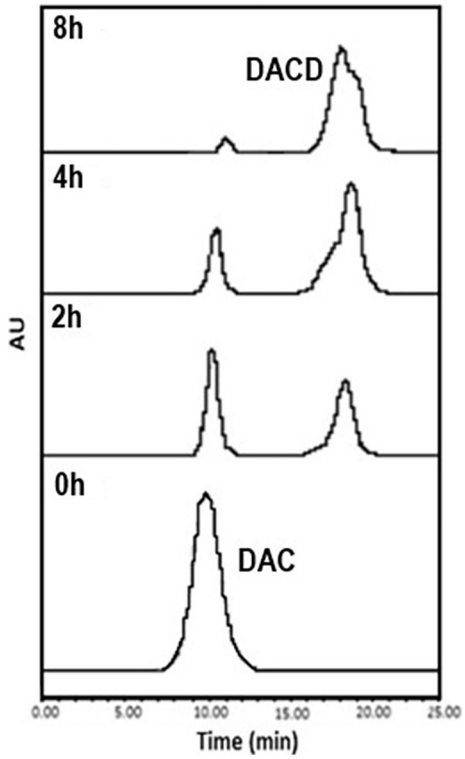

Fig. 3. HPLC-DAD chromatograms of the *in vitro* [4 + 2] photocycloaddition of DAC in methanolic solution under germicidal light.

[4 + 2] cycloadditions has been known for a long time ago, since the first one was isolated and purified from the fungus *Alternaria solani* [23–25]. Although, to the best of our knowledge, no Diels-Alderase enzymes catalyzing the formation of diterpenoid dimers have been reported until now.

3.4. DAC and DACD Scavenging Activities

Plants are susceptible to changes in UV radiation. Many of their principal physiological and biochemical processes involve RNS and ROS as central signaling molecules in both, stress and non-stress situations [26,27]. However, under adverse environmental conditions the concentration of these species in plant cells increases causing damage to biomolecules. The disruption in the equilibrium of ROS and RNS production and scavenging dictates (in conjunction with other factors) the plants ultimate physiological responses. Taking into account that in *B. flabellata* DACD appearance could be due to DAC dimerization likely catalyzed by light, we assessed on the scavenger activity of both compounds, DAC and DACD, toward ROS and RNS.

3.4.1. General Scavenging Activity toward Free Radicals

The first approach for evaluating the scavenging potential DAC and DACD was assessed by using the stable free radical DPPH. As it can be seen in Fig. 4A both, DAC and DACD are able to act as radical scavengers, producing a 75% and 95% of inhibition, respectively.

3.4.2. ROS Scavenging Activity

With the aim to evaluate the singlet oxygen ($^1O_2$) and superoxide radical ($\cdot O_2^-$) scavenging potential of DAC and DACD the delay in the photodegradation of riboflavin (Rf) in aqueous solutions was examined. When Rf absorbs visible light, several ROS are formed due to the presence of Rf triplet state ($^3Rf^*$). The main ones are $^1O_2$, produced with a quantum yield of 0.49, and $O_2\cdot^-$, generated with a low quantum yield (0.009); both cause the photochemical degradation of Rf [21]. Fig. 4B depicts superoxide radical inhibition. Rf degradation rate ($K_{obs}Rf$) mediated by $^1O_2$ oxidation decreases almost nine times when DACD is added to the photoreaction media. Nevertheless, DAC scavenger activity over natural degradation of Rf (almost 50% of Rf photoquenching) is similar to the one of ascorbic acid (AA) typically used as positive control. Moreover, $O_2\cdot^-$ scavenger activity of both terpene metabolites was higher than that shown by AA. Also, in this case the dimer is almost twice as effective as the monomer. Fig. 4C shows singlet oxygen inhibition.

3.4.3. RNS Scavenging Activity

Finally, nitric oxide radical (NO·) scavenging activities of both secondary metabolites were determined. IC_{50} values were 20.0 μg mL^{-1} and 6.0 μg mL^{-1} for the monomer and the dimer respectively; while AA only reached and IC_{50} = 41.0 μg mL^{-1}. Once again, both DAC and DACD were efficient in trapping NO·, although dimerization seemed to enhance the scavenging activity (Fig. 4D).

4. Conclusions

The dimerization of *ent*-15,16-epoxy-19-hydroxy-1,3,13(16),14-clerodatetraen-18-oic acid (DAC) is a process that is likely induced by solar radiation in *Baccharis flabellata* Hook. & Arn. var. *flabellata* aerial organs, although there is insufficient evidence to rule out the participation of enzymes. DACD is a dimeric compound that can be obtained *in vitro* from DAC by [4 + 2] photocycloaddition. *In vivo* accumulation of DACD throughout a complete *B. flabellata* phenological cycle is parallel to the increase in the intensity of solar radiation, if monomer is available. ROS and RNS scavenger abilities of both, the monomer and the dimer, were demonstrated, so it is thinkable that they could be

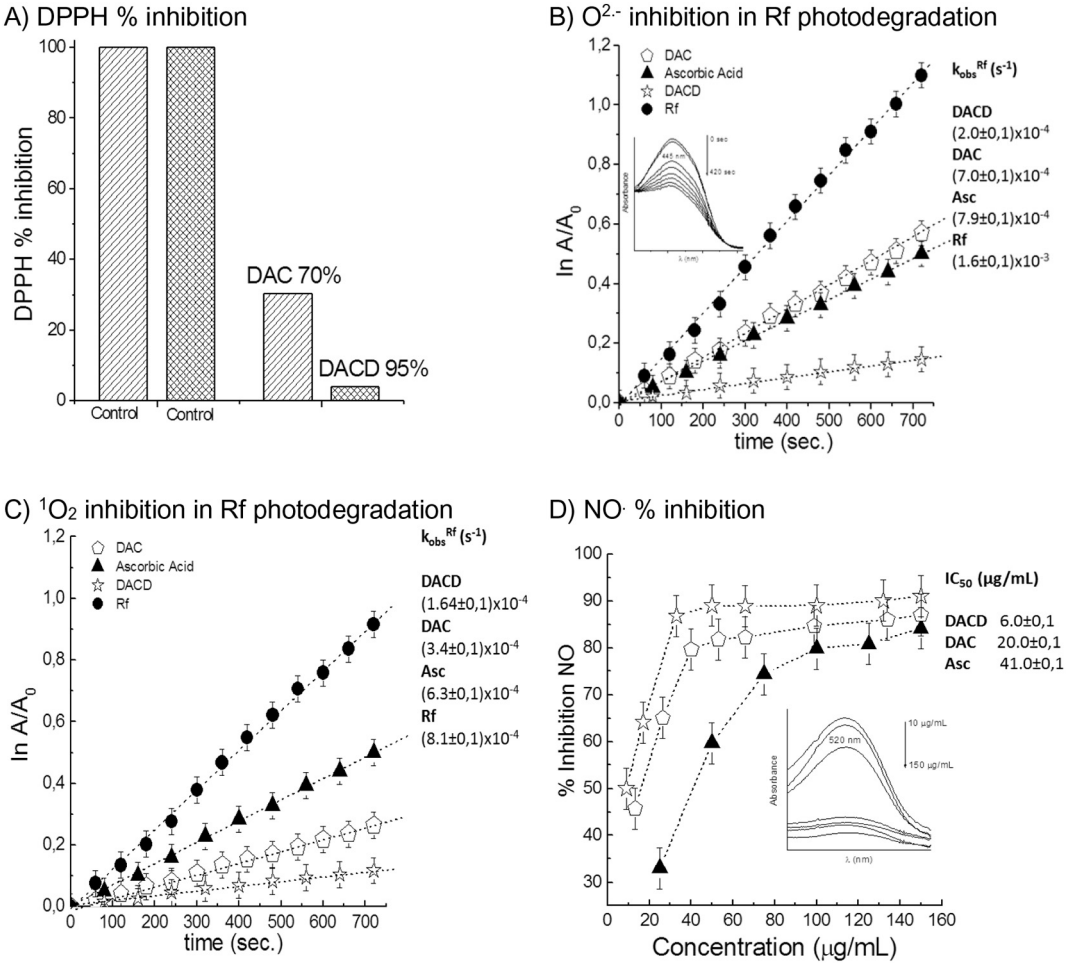

Fig. 4. DAC and DACD scavenger activities. A) DPPH % inhibition. B) $O^{2\cdot -}$ inhibition in Rf photodegradation. C) $^1O_2$ inhibition in Rf photodegradation. D) NO· % inhibition.

protectors toward photochemical oxidation. This is a new evidence of the fundamental role played by plant secondary metabolites as defense tools against adverse conditions such as radiation, in addition to their well-known allelochemical properties.

Conflict of Interest

The authors do not have any conflict of interest.

Acknowledgements

This work was supported by grants from UNSL (PROICO 2-1716), CONICET (PIP 2015-090) and ANPCyT (PICT 2014-0654); M.K.S, C.E.T. and M.F. are members of the Research Career of CONICET. Authors thank Lic. Monica Ferrari for technical assistance.

Appendix A. Supplementary Data

Supplementary data to this article can be found online at https://doi.org/10.1016/j.jphotobiol.2018.06.020.

References

[1] C.E. Tonn, O.S. Giordano, A new furane diterpenoid from Baccharis crispa Spr, An. Asoc. Quim. Argent. 68 (1980) 237–239.
[2] F. Bohlmann, S. Banerjee, J. Jalupovic, M. Grenz, L.N. Misra, G.S. Hirschmann, R.M. King, H. Robinson, Clerodane and labdane diterpenoids from Baccharis species, Phytochemistry 24 (1985) 511–515, https://doi.org/10.1016/S0031-9422(00)80758-X.
[3] J. Jakupovic, A. Schuster, U. Ganzer, F. Bohlmann, P.E. Boldt, Sesqui- and diterpenes from Baccharis species, Phytochemistry 29 (1990) 2217–2222, https://doi.org/10.1016/0031-9422(90)83041-X.
[4] V.E. Juan Hikawczuk, P.C. Rossomando, O.S. Giordano, J.R. Saad, *neo*-Clerodane diterpenoids from *Baccharis flabellata*, Phytochemistry 61 (2002) 389–394, https://doi.org/10.1016/S0031-9422(02)00241-8.
[5] J.R. Saad, J.G. Davicino, O.S. Giordano, A diterpene and flavonoids of *Baccharis flabellata*, Phytochemistry 27 (1988) 1884–1887, https://doi.org/10.1016/0031-9422(88)80471-0.
[6] T.G. Payne, P.R. Jefferies, The chemistry of Dodonaea spp-IV diterpene and flavonoid components of D. attenuate, Tetrahedron 29 (1973) 2575–2583.
[7] S. Dai, L. Zhang, K. Xiao, Q. Han, New cytotoxic *neo*-clerodane diterpenoids from Scutellaria strigillosa, Bioorg. Med. Chem. Lett. 26 (2016) 1750–1753, https://doi.org/10.1016/j.bmcl.2016.02.045.
[8] A.A. El-Hela, N.M. Abdel-Hady, G.T.M. Dawoud, M.M. Ghoneim, HPTLC fingerprint profile of triterpenes of Lamium amplexicaule Benth. and Ajuga iva L. (Lamiaceae) monitored with screening of their anti-inflammatory effect, J. Pharmacogn. Phytochem. 5 (2016) 176–181.
[9] R.A. Raccuglia, G. Bellone, K. Loziene, F. Piozzi, S. Rosselli, A. Maggio, M. Bruno, M.S.J. Simmonds, Hastifolins A-G, antifeedant *neo*-clerodane diterpenoids from Scutellaria hastifolia, Phytochemistry 71 (2010) 2087–2091, https://doi.org/10.1016/j.phytochem.2010.08.021.
[10] M.E. Sosa, C.E. Tonn, Plant secondary metabolites from Argentinean semiarid lands: bioactivity against insects, Phytochem. Rev. 7 (2008) 3–24, https://doi.org/10.1007/s11101-006-9056-7.
[11] R. Li, S.L. Morris-Natschkeb, K.H. Lee, Clerodane diterpenes: sources, structures, and biological activities, Nat. Prod. Rep. 33 (2016) 1121–1122, https://doi.org/10.1039/C5NP00137D.
[12] E. Gravel, E. Poupon, Biogenesis and biomimetic chemistry: can complex natural products be assembled spontaneously? Eur. J. Org. Chem. 2008 (2008) 27–42, https://doi.org/10.1002/ejoc.200790103.
[13] G.L. Lin, C.O. Ung, Z.L. Feng, L. Huang, H. Hu, Naturally occurring diterpenoid dimers: source, biosynthesis, chemistry and bioactivities, Planta Med. 82 (2016) 1309–1328, https://doi.org/10.1055/s-0042-114573.
[14] Z. Pan, D. Ning, X. Wu, S. Huang, D. Li, S. Lv, New clerodane diterpenoids from the twigs and leaves of Croton Euryphyllus, Bioorg. Med. Chem. Lett. 25 (2015)

1329–1332, https://doi.org/10.1016/j.bmcl.2015.01.033.
[15] B.R. Jordan, The effects of ultraviolet-B radiation on plants: a molecular perspective, Adv. Bot. Res. 22 (1996) 97–162, https://doi.org/10.1016/S0065-2296(08)60057-9.
[16] M.A.K. Jansen, V. Gaba, B.M. Greenberg, Higher plants and UV-B radiation: balancing damage, repair and acclimation, Trends Plant Sci. 3 (1998) 131–135, https://doi.org/10.1016/S1360-1385(98)01215-1.
[17] V. Tossi, L. Lamattina, R. Cassia, An increase in the concentration of abscisic acid is critical for nitric oxide-mediated plant adaptive responses to UV-B irradiation, New Phytol. 181 (2009) 871–879, https://doi.org/10.1111/j.1469-8137.2008.02722.x.
[18] S. Mackerness A-H, C.F. John, B. Jordan, B. Thomas, Early signaling components in ultraviolet-B responses: distinct roles for different reactive oxygen species and nitric oxide, FEBS Lett. 489 (2001) 237–242, https://doi.org/10.1016/S0014-5793(01)02103-2.
[19] M. Zhang, J.F. Dong, H.H. Jin, L.N. Sun, M.J. Xu, Ultraviolet-B-induced flavonoid accumulation in Betula pendula leaves is dependent upon nitrate reductase-mediated nitric oxide signaling, Tree Physiol. (8) (2011) 798–807, https://doi.org/10.1093/treephys/tpr070.
[20] D.Q. Falcão, E.R. Costa, D.S. Alviano, C.S. Alviano, R.M. Kuster, F.S. Menezes, Atividade antioxidante e antimicrobiana de Calceolaria chelidonioides Humb. Bonpl. & Kunth, Braz. J. Pharmacogn. 16 (2006) 73–76 http://www.scielo.br/pdf/rbfar/v16n1/a12v16n1.
[21] F. Wilkinson, W.P. Helman, A.B. Ross, Quantum yields for the photosensitised formation of the lowest electronically excited singlet state if molecular oxygen in solution, J. Phys. Chem. Ref. Data 22 (1993) 113–262, https://doi.org/10.1063/1.555934.
[22] B. Pang, G. Zhong, Z. Tang, W. Liu, Enzymatic [4 + 2] cycloadditions in the biosynthesis of spirotetramates and spirotetronates, Methods Enzymol. 575 (2016) 39–63, https://doi.org/10.1016/bs.mie.2016.02.019.
[23] H. Oikawa, T. Tokiwano, Enzymatic catalysis of the Diels-Alder reaction in the biosynthesis of natural products, Nat. Prod. Rep. 21 (2004) 321–352, https://doi.org/10.1039/B305068H.
[24] H. Oikawa, Involvement of the Diels-Alderases in the biosynthesis of natural products, B. Chem. Soc. Jpn. 78 (2005) 537–554, https://doi.org/10.1246/bcsj.78.537.
[25] K. Katayama, T. Kobayashi, H. Oikawa, M. Honma, A. Ichihara, Enzymatic activity and partial purification of solanapyrone synthase: first enzyme catalyzing Diels-Alder reaction, Biochim. Biophys. Acta 1384 (1998) 387–395, https://doi.org/10.1016/S0167-4838(98)00040-5.
[26] A. Besson-Bard, A. Pugin, D. Wendehenne, New insights into nitric oxide signaling in plants, Annu. Rev. Plant Biol. 59 (2008) 21–39, https://doi.org/10.1146/annurev.arplant.59.032607.092830.
[27] M.A. Torres, ROS in biotic interactions, Physiol. Plant. 138 (2010) 414–429, https://doi.org/10.1111/j.1399-3054.2009.01326.x.